

Disentangling stopped proton and inclusive net-proton fluctuations at RHIC

D. K. Mishra^{1,*} and P. Garg^{2,†}

¹*Nuclear Physics Division, Bhabha Atomic Research Center, Mumbai 400085, India*

²*Department of Physics and Astronomy, Stony Brook University,
SUNY, Stony Brook, New York 11794-3800, USA*

The recent results on net-proton and net-charge multiplicity fluctuations from the beam energy scan program at RHIC have drawn much attention to explore the critical point in the QCD phase diagram. Experimentally measured protons contain contribution from various processes such as secondaries from higher mass resonance decay, production process, and protons from the baryon stopping. Further, these contributions also fluctuate from event to event and can contaminate the dynamical fluctuations due to the critical point. We present the contribution of stopped proton and produced proton fluctuations in the net-proton multiplicity fluctuation in Au+Au collisions measured by STAR experiment at RHIC. The produced net-proton multiplicity fluctuations using cumulants and their ratios are studied as a function collision energies. After removing the stopped proton contribution from the inclusive proton multiplicity distribution, a non-monotonic behavior is even more pronounced in the net-proton fluctuations around $\sqrt{s_{NN}} = 19.6$ GeV, both in $S\sigma$ and $\kappa\sigma^2$. The present study will be useful to understand the fluctuations originating due to critical point.

PACS numbers: 25.75.Gz,12.38.Mh,21.65.Qr,25.75.-q,25.75.Nq

I. INTRODUCTION

The recent Beam Energy Scan (BES) program at Relativistic Heavy Ion Collider (RHIC) is motivated to explore the structure of QCD phase diagram, such as a first order co-existence region or a critical point [1–4]. Lattice QCD calculations suggest that, there is a simple cross-over from quark-gluon-plasma (QGP) to hadronic phase at high T and low μ_B [5–7]. Several other models predict a first order phase transition at large μ_B and low T [8, 9]. Hence, there should be a point where the first order phase transition line ends, which is named as QCD critical end point (CEP) [10, 11].

The moments (mean M , variance σ , skewness S , and kurtosis κ) of the multiplicity distribution of conserved quantities such as, net-baryon, net-charge, and net-strangeness are related to the correlation length (ξ) of the system [1, 2]. Hence, event-by-event fluctuations of these conserved quantities can be used to look for signals of a critical point and phase transition [12–14]. Most of the experimental efforts are made to measure the fluctuations in terms of moments or cumulants of above conserved quantities. The higher moments have stronger dependence on ξ , thus should be more sensitive to the critical fluctuations, originating due to phase transition trajectory that passes through a critical point [2, 10, 11, 14–16]. The individual moments (cumulants C_n , $n = 1, 2, 3$, and 4) of the conserved distributions can have trivial system dependence, which can be minimized by taking the ratios of the moments. Further, the cumulant ratios can be related to the generalized susceptibilities calculated in

lattice QCD [9, 10, 16] and other statistical model calculations [17–19].

The experiments at RHIC have reported the results on higher moments of net-proton [20, 21] and net-charge [22, 23] multiplicity distributions, using the data from BES-I program at different center of mass energies ($\sqrt{s_{NN}} = 7.7, 11.5, 19.6, 27, 39, 62.4$, and 200 GeV. At lower collision energies, the STAR experiment observed a large deviation from the Poisson expectation in the net-proton fluctuation results [21]. Several studies have been performed to estimate the sources of excess fluctuations, such as the effect of kinematical acceptance [18], volume fluctuations [4], inclusion of resonance decays [24–26], exact (local) charge conservation [27–29] or repulsive vander-Walls forces among hadrons [30, 31]. The effect of baryon stopping is predominant at lower collision energies, where a possible QCD critical point is expected to be observed. The proton and anti-proton pair-production is negligible at lower $\sqrt{s_{NN}}$, hence most of the measured protons are originated from the beam particles. Therefore, the dynamics of baryon stopping is another source of fluctuation, which can distort the signal for the critical point and phase-transition [32]. However, it is important to estimate the fluctuations due to baryon stopping and initial state participant fluctuations [33].

The experimentally observed baryon stopping could be used as a direct tool to explore the QCD phase transition [34]. The stopping in nuclear collision can be estimated from the rapidity loss occurred by the baryons. Hence, baryon stopping is inferred through the net-baryon rapidity (y) distribution [34]. The measured net-baryon distribution retains the information about the energy loss and allows to determine the degree of nuclear stopping. The baryon stopping can be quantified by the reduced curvature of the net-proton rapidity distribution at mid-rapidity. Since most of the experiment do not

*Electronic address: dkmishra@rcf.rhic.bnl.gov

†Electronic address: prakhar@rcf.rhic.bnl.gov

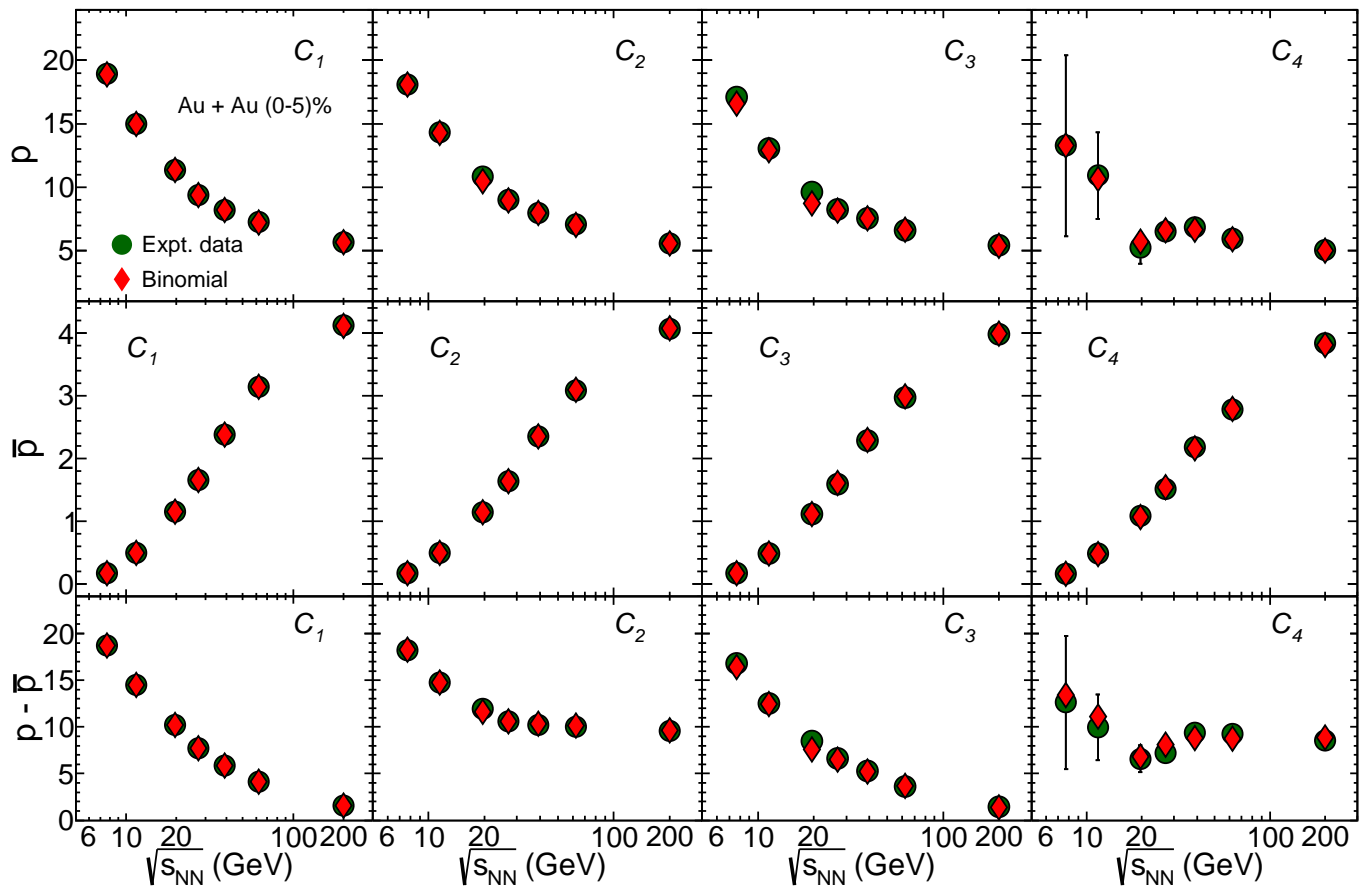


FIG. 1: The efficiency corrected individual cumulants of inclusive protons (p), anti-protons (\bar{p}), and net-protons ($p - \bar{p}$) multiplicity as a function of $\sqrt{s_{NN}}$ in most central (0%–5%) Au+Au collisions. The experimental cumulants from [21, 41] are compared with the same obtained from a Binomial assumption.

measure neutrons within the same kinematical acceptance as protons, hence baryon stopping can be accessible through the measurement of protons and anti-protons. Further, the measured protons have contributions from both stopping and produced protons. At AGS energies, the number of produced anti-proton is very small, the net-baryon rapidity distribution is similar to the proton distribution [35–37]. At SPS energies, the net-proton rapidity distribution shows a double hump structure with a dip around $y = 0$. This suggests that, the reaction at SPS is beginning to be transparent, only small fraction of original baryons are found at the mid-rapidity and the hump structures reflect the rapidity distributions of the produced protons after the collisions [38]. At RHIC, the rapidity distribution for net-protons at $\sqrt{s_{NN}} = 200$ GeV is different from those at lower energies indicating a different system formed around the mid-rapidity [39]. The experimental data shows that collisions at such high energy exhibit a high degree of transparency. Baryon transparency, which is inverse of baryon stopping, increases with the collision energy. Since baryon stopping plays a major role at lower $\sqrt{s_{NN}}$, which almost vanishes at higher collision energies, it is important to disentangle

the contribution of stopped baryons and the produced baryons in order to understand the QCD phase structure and critical point.

The present work is motivated to study the net-proton multiplicity fluctuation, which is related to the particle production mechanism. Experimentally measured proton (anti-proton) multiplicity distributions contain the contributions from nuclear stopping, resonance decay, and also directly produced from the collisions. A detailed studies of resonance contribution to net-proton fluctuations have been reported in Refs. [24, 25]. The previous net-proton fluctuation studies [20, 21] by STAR experiment have been performed by using higher moments with inclusive proton (anti-proton) multiplicity distributions. However, after subtracting the stopping contribution from the inclusive proton multiplicity distribution, it may have large effect in the correlation of proton and anti-proton multiplicities. This can affect the higher moments of the net-proton multiplicity fluctuations [40]. It will be interesting to look for higher moments of net-proton fluctuations after removing the stopped proton contribution, which is dominant at lower $\sqrt{s_{NN}}$.

The paper is organized as follows: In the following sec-

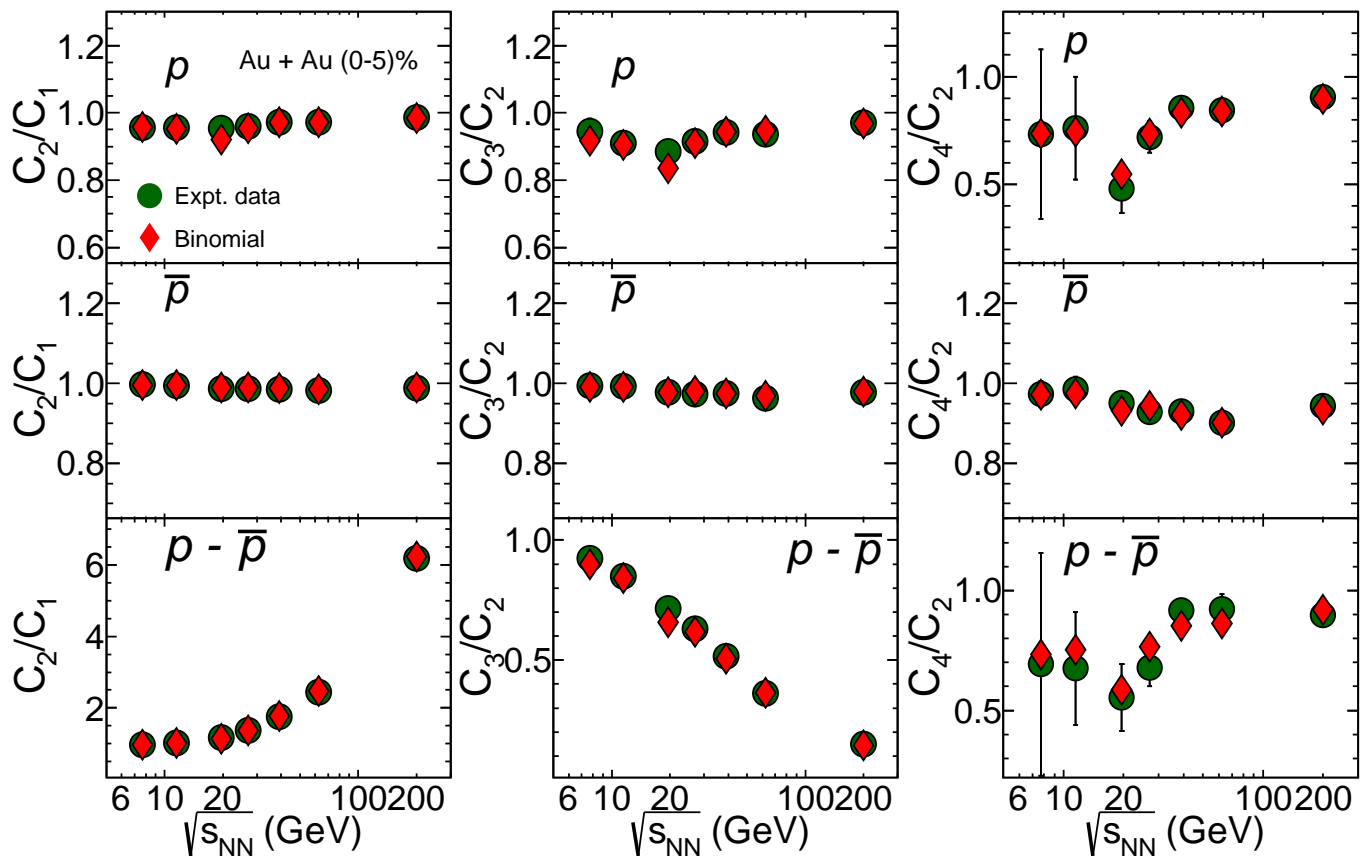


FIG. 2: Collision energy dependence of efficiency corrected cumulant ratios (C_2/C_1 , C_3/C_2 , and C_4/C_2) of p , \bar{p} , and $p - \bar{p}$ as a function of $\sqrt{s_{NN}}$ in most central (0%–5%) Au+Au collisions. The experimental cumulant ratios from [21, 41] are compared with the same obtained from a Binomial assumption.

tion, we discuss the method used for the present study. In Sec. III, the results of individual contribution to the proton fluctuations and net-proton fluctuations are shown. Finally, we summarize our work and discuss its implications in Sec. IV.

II. METHOD

The STAR experiment at RHIC reported the results on the cumulants and their ratios of the net-protons multiplicity distributions at various collision energies [21] by measuring the number of proton and anti-proton multiplicities on an event-by-event basis. As mentioned in the previous section, the measured protons (p^{incl}) have contributions from the stopped protons (p^{stop}) and produced protons (p^{prod}). In the present work, we make an attempt to estimate the contributions of stopped and produced proton to the net-proton fluctuation results.

A Monte-Carlo approach is adopted by taking two independent distributions of proton (p^{incl}) and anti-proton (\bar{p}) multiplicities as Binomial distribution. The mean values used in the Binomial distribution of p^{incl} and \bar{p} for (0% – 5%) centrality in Au+Au collisions at differ-

ent $\sqrt{s_{NN}}$ are taken from Refs. [21, 41], also shown in Table I. The net-proton multiplicity p^{diff} ($= p^{\text{incl}} - \bar{p}$) distribution is then constructed from independently produced p^{incl} and \bar{p} distributions. For the proof of principle, we calculate the individual cumulants of measured proton, anti-proton and net-proton multiplicities, which are distributed binomially and compare them with the experimentally measured cumulants. Also, by this construction, we get access to the efficiency corrected distributions of protons and anti-protons.

Figure 1 shows comparison of experimentally measured individual cumulants for proton, anti-proton, and net-proton multiplicity distributions for (0% – 5%) centrality in Au+Au collisions with the same obtained from Binomial expectation. It is to be noted that, the experimentally measured cumulants are corrected for reconstruction efficiency and finite centrality bin width correction. We tried simultaneously to reproduce all the cumulants (C_1 , C_2 , C_3 , and C_4) at each $\sqrt{s_{NN}}$ using the binomially distributed p^{incl} and \bar{p} . Also the cumulants for net-proton multiplicity distributions are well reproduced at each collision energy. Figure 2 shows the cumulant ratios (C_2/C_1 , C_3/C_2 , and C_4/C_2) of p , \bar{p} , and net-proton multiplicities

TABLE I: Mean values of inclusive proton, anti-proton, and stopped proton distributions for most central (0%–5%) Au+Au collisions at various $\sqrt{s_{NN}}$ measured by STAR experiment [21, 33, 41].

$\sqrt{s_{NN}}$ (GeV)	7.7	11.5	19.6	27	39	62.4	200
Incl. proton	18.918 ± 0.009	15.005 ± 0.006	11.375 ± 0.003	9.390 ± 0.002	8.221 ± 0.001	7.254 ± 0.002	5.664 ± 0.001
anti-proton	0.165 ± 0.001	0.490 ± 0.001	1.150 ± 0.001	1.652 ± 0.001	2.379 ± 0.001	3.135 ± 0.001	4.116 ± 0.001
stopped proton	17.21 ± 0.86	12.89 ± 0.86	9.73 ± 0.80	7.61 ± 0.73	5.78 ± 0.65	3.78 ± 0.54	1.54 ± 0.33

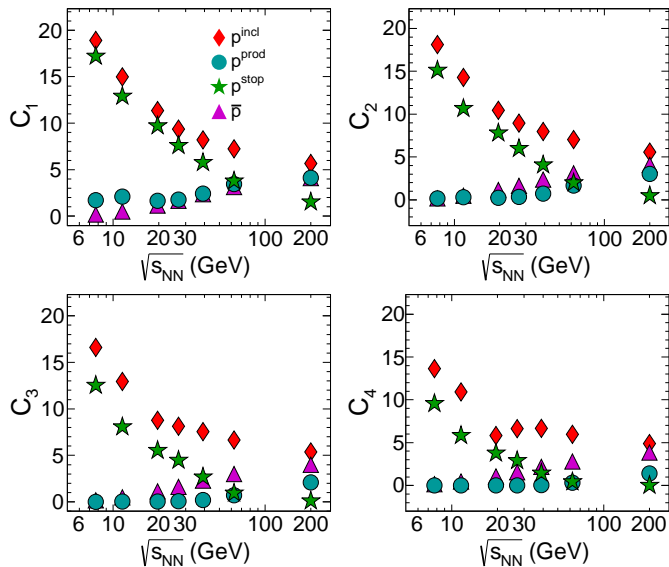


FIG. 3: Collision energy dependence of cumulants C_1 , C_2 , C_3 , and C_4 of inclusive protons (p^{incl}), produced protons (p^{prod}), stopped protons (p^{stop}), and anti-protons in most central (0%–5%) Au+Au collisions obtained from Binomial distributions.

at different $\sqrt{s_{NN}}$, which are calculated from the individual cumulants shown in Fig. 1. Hence, it is established that, using the Binomial distribution, the cumulant ratios are also well reproduced at each collision energy for p , \bar{p} , and net-proton cases. The maximum deviation, which was observed in experimental data for C_4/C_2 values of proton and net-proton cases at $\sqrt{s_{NN}} = 19.6$ GeV are also well reproduced. In the remaining study of this paper, we have used the above Binomial distributions which describe all the efficiency corrected cumulants and their ratios of the experimental net-proton data. In the real experimental situation, it is difficult to correct the efficiency of the proton, anti-proton and net-proton multiplicity distributions on an event-by-event basis. Hence, using the above method, one can obtain the efficiency corrected multiplicity distributions.

The widely discussed net-proton fluctuation study by STAR experiment has contribution from inclusive proton and produced anti-protons. Further, the inclusive protons ($p^{\text{incl}} = p^{\text{stop}} + p^{\text{prod}}$) have contributions from both stopped protons and produced protons. Whereas stopping has no contribution to the anti-proton production,

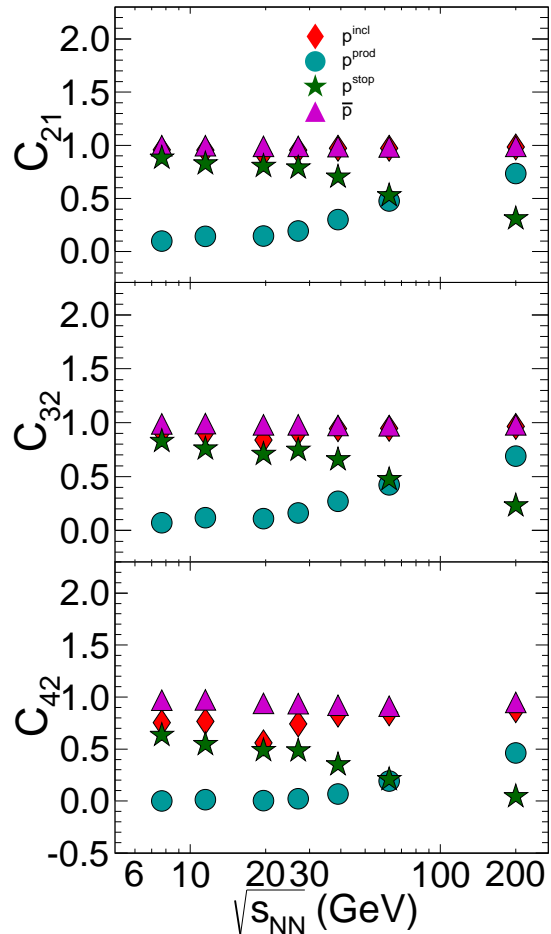


FIG. 4: Collision energy dependence of cumulant ratios (C_2/C_1 , C_3/C_2 , C_4/C_2 , and C_3/C_1) of p^{incl} , p^{prod} , p^{stop} , and anti-protons in most central (0%–5%) Au+Au collisions obtained from Binomial distributions.

they come from resonance decay and produced particles in the collisions. The mean number of stopped protons p^{stop} at various BES energies have been estimated using net-proton rapidity distributions for the most central collisions measured by different experiments [33]. The reported p^{stop} values are in the same kinematical acceptance (transverse momentum $0.4 \leq p_T$ (GeV/c) ≤ 0.8 and pseudo-rapidity $|\eta| < 0.5$) as the STAR experimental data, therefore they are used directly in the present study.

Experimentally, it is not trivial to tag a measured pro-

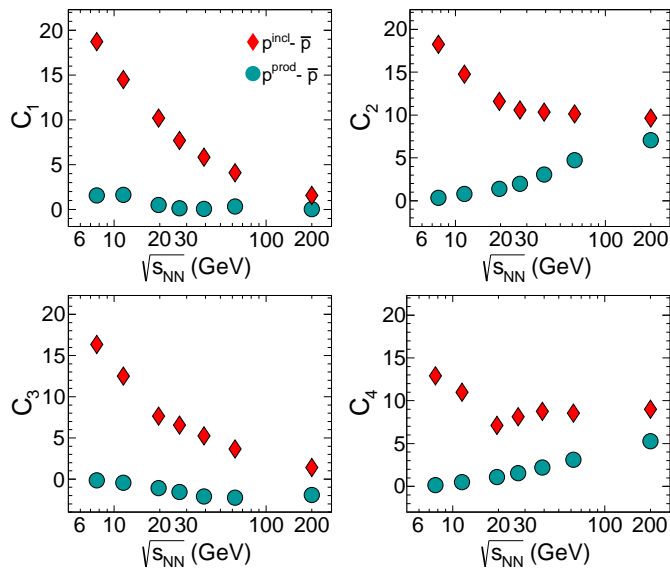


FIG. 5: Variation of cumulants of net-proton multiplicity distributions as a function of $\sqrt{s_{NN}}$ in most central (0%–5%) Au+Au collisions obtained from Binomial assumption. The net-proton multiplicity distributions are calculated by taking $p^{\text{incl}} - \bar{p}$ and $p^{\text{prod}} - \bar{p}$ distributions, assuming individual p^{incl} and \bar{p} distributions as Binomial.

ton originating from stopping or production, hence, the correction for the stopped protons to the net-proton multiplicity distribution can not be applied to the experimental measurement. The fraction of stopped and produced proton contributions in the inclusive proton distribution are estimated by taking the mean number of p^{incl} [41] and p^{stop} [33]. The stopped and produced proton fractions are calculated as: $f^{\text{stop}} = (C_1 \text{ of } p^{\text{stop}} / C_1 \text{ of } p^{\text{incl}})$ and $f^{\text{prod}} = [(C_1 \text{ of } p^{\text{incl}} - C_1 \text{ of } p^{\text{stop}}) / C_1 \text{ of } p^{\text{incl}}]$, respectively. The stopped proton and produced proton distributions are constructed on event-by-event basis from the inclusive proton distribution weighted by corresponding f^{stop} and f^{prod} fractions, respectively. Hence, the mean of the original p^{incl} distribution change to the corresponding mean values of p^{stop} and p^{prod} , without modifying the shape of the distribution. The resulting p^{stop} and p^{prod} distributions also remain Binomial. These factorized multiplicity distributions along with the anti-proton multiplicity distributions are further used for the study of net-proton fluctuation at various collision energies.

III. RESULTS AND DISCUSSIONS

The cumulants are calculated from the reconstructed p^{incl} , p^{stop} , and p^{prod} distributions. Figure 3 shows the individual cumulants (C_1 , C_2 , C_3 , and C_4) of the inclusive proton, produced proton, stopped proton, and anti-proton multiplicity distributions as a function of center of mass energy obtained from the Binomial distributions

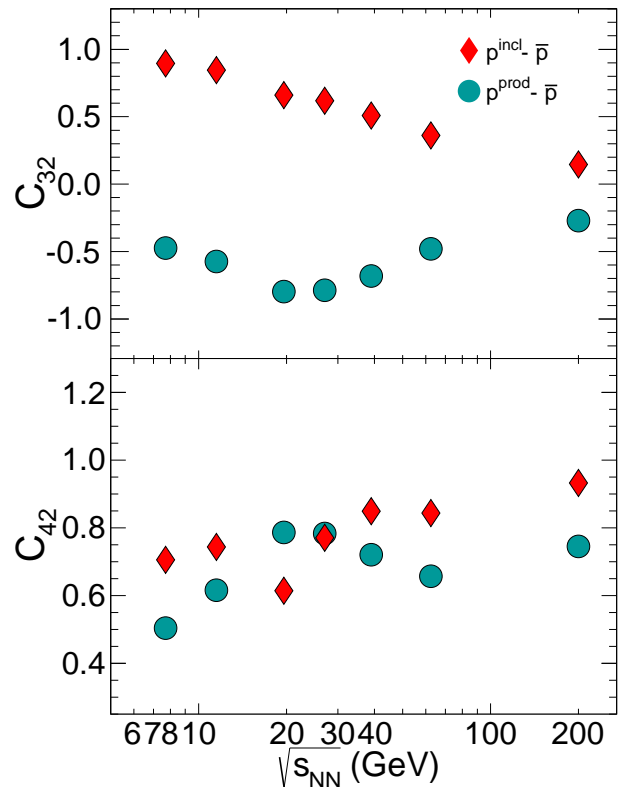


FIG. 6: Variation of cumulant ratios C_3/C_2 and C_4/C_2 of net-proton distributions as a function of $\sqrt{s_{NN}}$ in most central (0–5%) Au+Au collisions obtained from Binomial assumption. The net-proton distributions are calculated by taking $p^{\text{incl}} - \bar{p}$ and $p^{\text{prod}} - \bar{p}$ distributions, assuming individual p^{incl} and \bar{p} distributions as Binomial.

as described in Sec. II. All the cumulants of p^{incl} decrease with increasing $\sqrt{s_{NN}}$ and the \bar{p} cumulants show opposite trend. At lower energies (below $\sqrt{s_{NN}} = 39$ GeV), the cumulants of p^{stop} and p^{incl} follow each other closely. This indicates that at lower energies, the dominant contribution to the p^{incl} fluctuation come from the p^{stop} . The cumulants of produced protons and the anti-protons follow close to each other, which further strengthen the argument. This behavior is consistent with the picture of evolution of baryon stopping and nuclear transparency with collision energies. Figure 4 shows the cumulant ratios (C_2/C_1 , C_3/C_2 , and C_4/C_2) for the above mentioned (p^{incl} , p^{stop} , p^{prod} , and \bar{p}) distributions as a function of $\sqrt{s_{NN}}$. As observed in experimental data, the cumulant ratios of p^{incl} and \bar{p} are similar except for the C_4/C_2 ratios at lower energies ($\sqrt{s_{NN}} < 39$ GeV). The cumulant ratios for p^{stop} and p^{prod} show opposite trend as a function of collision energy. The baryon stopping contribution decreases with increasing collision energies, whereas the produced proton contribution increases. The individual cumulants and their ratios for p^{prod} and p^{stop} match at $\sqrt{s_{NN}} = 62.4$ GeV, indicating the contribution from the stopping and the produced protons is almost similar to

the inclusive proton production. Further, this may also indicate that, there is equal contribution to the nuclear stopping and transparency in rapidity space at $\sqrt{s_{NN}} = 62.4$ GeV [42] in STAR acceptance.

The net-proton p^{diff} cumulants are obtained by taking the number of p^{incl} and \bar{p} multiplicity distributions on an event-by-event basis. We have also estimated the net-proton cumulants of the produced particles by taking the p^{prod} and \bar{p} multiplicity distributions. Figure 5 shows the individual cumulants of net-proton multiplicity distribution as a function of $\sqrt{s_{NN}}$. The cumulants of the difference distribution obtained from $p^{\text{incl}} - \bar{p}$ decrease as a function of collision energy. As can be observed in Fig.3, after subtracting the stopping contributions from the p^{incl} distribution, the average number of produced protons and anti-protons are similar, which gives a smaller value of C_1 in $p^{\text{prod}} - \bar{p}$ distribution and it is independent of collision energy. The cumulants (C_1 and C_3) of the difference distributions obtained from $p^{\text{prod}} - \bar{p}$ multiplicities show small energy dependence, whereas C_2 and C_4 cumulants systematically increase with $\sqrt{s_{NN}}$. Figure 6 shows the energy dependence of ratios of cumulants (C_3/C_2 and C_4/C_2) for net-proton p^{diff} distributions obtained from p^{incl} , p^{prod} , and \bar{p} multiplicity distributions. The C_3/C_2 ratios of net-proton distributions by taking inclusive protons and anti-protons decrease with collision energies, similar observation is also reported by STAR experiment [21]. Further, the C_3/C_2 ratios from the produced protons and anti-protons as a function of $\sqrt{s_{NN}}$, are found to be minimum around 19.6 GeV. The C_4/C_2 ($= \kappa\sigma^2$) ratios from $p^{\text{incl}} - \bar{p}$ shows deviation from the Poisson expectation for lower collision energies and maximum deviation is observed at 19.6 GeV, which is also observed in the experimental data. The C_4/C_2 ratios obtained from $p^{\text{prod}} - \bar{p}$ increase with $\sqrt{s_{NN}}$ up to 19.6 GeV and remain constant there after. While taking the inclusive proton with \bar{p} , a minimum is observed at 19.6 GeV for C_4/C_2 ratios, whereas by taking the produced proton and anti-proton a maximum is observed at the same energy. After removing the stopping contribution from the inclusive proton distribution, the C_3/C_2

and C_4/C_2 ratios of the net-proton (p^{diff}) multiplicity distribution shows non-monotonic behavior at $\sqrt{s_{NN}} = 19.6$ GeV, which may indicate the presence of a critical point or phase-transition in heavy-ion collisions.

IV. SUMMARY

To summarize the present work, we demonstrate a method to disentangle the contribution of the stopped protons and produced protons from the inclusive proton fluctuations in the heavy-ion collisions. The $\sqrt{s_{NN}}$ dependence of the efficiency corrected cumulants and their ratios for proton, anti-proton, and net-proton multiplicities are compared with the same obtained from a Binomial distributions. The individual cumulants and their ratios for p^{incl} , p^{prod} , p^{stop} , and \bar{p} are studied as a function of collision energy. At lower collision energies, the p^{incl} fluctuations are dominated by p^{stop} and at higher energies they are dominated by produced proton fluctuations. The contribution from stopping and produced protons to the inclusive proton fluctuations at $\sqrt{s_{NN}} = 62.4$ GeV are similar. The net-proton fluctuations calculated using $p^{\text{incl}} - \bar{p}$ and $p^{\text{prod}} - \bar{p}$ distributions are studied as a function of $\sqrt{s_{NN}}$. All the individual cumulants from $p^{\text{incl}} - \bar{p}$ decrease with $\sqrt{s_{NN}}$. The C_1 and C_3 of $p^{\text{prod}} - \bar{p}$ remain constant as a function of $\sqrt{s_{NN}}$. The C_2 and C_4 values increase with collision energies. The cumulants ratios C_3/C_2 and C_4/C_2 are studied as a function of collision energies for the above two different net-proton cases. There is a minimum observed in C_4/C_2 ratio at $\sqrt{s_{NN}} = 19.6$ GeV for net-proton distribution using the inclusive proton. Whereas, after removing the stopping contribution from the inclusive proton distribution, the C_3/C_2 and C_4/C_2 ratios of the net-proton multiplicity distribution shows non-monotonic behavior around $\sqrt{s_{NN}} = 19.6$ GeV. This may indicate the presence of a critical point or a phase-transition in high-energy heavy-ion collisions. This is a first such attempt to separate the stopped and produced proton fluctuations from the net-proton fluctuations.

-
- [1] M. A. Stephanov, K. Rajagopal and E. V. Shuryak, Phys. Rev. Lett. **81**, 4816 (1998).
 - [2] M. A. Stephanov, Phys. Rev. Lett. **102**, 032301 (2009).
 - [3] M. Kitazawa, M. Asakawa and H. Ono, Phys. Lett. B **728**, 386 (2014).
 - [4] V. Skokov, B. Friman and K. Redlich, Phys. Rev. C **88**, 034911 (2013).
 - [5] Y. Aoki, G. Endrodi, Z. Fodor, S. D. Katz and K. K. Szabo, Nature **443**, 675 (2006).
 - [6] Z. Fodor and S. D. Katz, JHEP **0404**, 050 (2004).
 - [7] M. G. Alford, K. Rajagopal and F. Wilczek, Phys. Lett. B **422**, 247 (1998).
 - [8] M. A. Stephanov, Prog. Theor. Phys. Suppl. **153**, 139 (2004), Int. J. Mod. Phys. A **20**, 4387 (2005).
 - [9] A. Bazavov, H. T. Ding, P. Hegde, O. Kaczmarek, F. Karsch, E. Laermann, S. Mukherjee and P. Petreczky *et al.*, Phys. Rev. Lett. **109**, 192302 (2012).
 - [10] S. Ejiri, F. Karsch and K. Redlich, Phys. Lett. B **633**, 275 (2006).
 - [11] M. A. Stephanov, K. Rajagopal and E. V. Shuryak, Phys. Rev. D **60**, 114028 (1999).
 - [12] V. Koch, A. Majumder and J. Randrup, Phys. Rev. Lett. **95**, 182301 (2005).
 - [13] M. Asakawa, U. W. Heinz and B. Muller, Phys. Rev. Lett. **85**, 2072 (2000).
 - [14] M. Asakawa, S. Ejiri and M. Kitazawa, Phys. Rev. Lett. **103**, 262301 (2009).
 - [15] R. V. Gavai and S. Gupta, Phys. Lett. B **696**, 459 (2011).

- [16] M. Cheng, P. Hegde, C. Jung, F. Karsch, O. Kaczmarek, E. Laermann, R. D. Mawhinney and C. Miao *et al.*, Phys. Rev. D **79**, 074505 (2009).
- [17] F. Karsch and K. Redlich, Phys. Lett. B **695**, 136 (2011).
- [18] P. Garg, D. K. Mishra, P. K. Netrakanti, B. Mohanty, A. K. Mohanty, B. K. Singh and N. Xu, Phys. Lett. B **726**, 691 (2013).
- [19] D. K. Mishra, P. K. Netrakanti and B. Mohanty, Phys. Rev. C **94**, 054906 (2016).
- [20] M. M. Aggarwal *et al.* [STAR Collaboration], Phys. Rev. Lett. **105**, 022302 (2010).
- [21] L. Adamczyk *et al.* [STAR Collaboration], Phys. Rev. Lett. **112**, 032302 (2014).
- [22] A. Adare *et al.* [PHENIX Collaboration], Phys. Rev. C **93**, 011901 (2016).
- [23] L. Adamczyk *et al.* [STAR Collaboration], Phys. Rev. Lett. **113**, 092301 (2014).
- [24] D. K. Mishra, P. Garg, P. K. Netrakanti and A. K. Mohanty, Phys. Rev. C **94**, 014905 (2016).
- [25] M. Nahrgang, M. Bluhm, P. Alba, R. Bellwied and C. Ratti, Eur. Phys. J. C **75**, no. 12, 573 (2015).
- [26] V. V. Begun, M. I. Gorenstein, M. Hauer, V. P. Konchakovski and O. S. Zozulya, Phys. Rev. C **74**, 044903 (2006).
- [27] A. Bzdak, V. Koch and V. Skokov, Phys. Rev. C **87**, 014901 (2013).
- [28] M. Nahrgang, T. Schuster, M. Mitrovski, R. Stock and M. Bleicher, Eur. Phys. J. C **72**, 2143 (2012).
- [29] P. K. Netrakanti, X. F. Luo, D. K. Mishra, B. Mohanty, A. Mohanty and N. Xu, Nucl. Phys. A **947**, 248 (2016).
- [30] J. Fu, Phys. Lett. B **722**, 144 (2013).
- [31] A. Bhattacharyya, R. Ray, S. Samanta and S. Sur, Phys. Rev. C **91**, no. 4, 041901 (2015).
- [32] A. Bzdak, V. Koch and V. Skokov, Eur. Phys. J. C **77**, 288 (2017).
- [33] D. Thakur, S. Jakhar, P. Garg and R. Sahoo, Phys. Rev. C **95**, 044903 (2017).
- [34] Y. B. Ivanov, Phys. Lett. B **690**, 358 (2010).
- [35] B. B. Back *et al.* [E917 Collaboration], Phys. Rev. Lett. **86**, 1970 (2001).
- [36] L. Ahle *et al.* [E802 Collaboration], Phys. Rev. C **60**, 064901 (1999).
- [37] J. Barrette *et al.* [E877 Collaboration], Phys. Rev. C **62**, 024901 (2000).
- [38] T. Anticic *et al.* [NA49 Collaboration], Phys. Rev. Lett. **93**, 022302 (2004).
- [39] I. G. Bearden *et al.* [BRAHMS Collaboration], Phys. Rev. Lett. **93**, 102301 (2004).
- [40] D. K. Mishra, P. Garg and P. K. Netrakanti, Phys. Rev. C **93**, 024918 (2016).
- [41] Cumulants of proton and anti-proton distribution measured by STAR experiment.
- [42] S. M. H. Wong, Phys. Lett. B **480**, 65 (2000).